Journal of Molecular Histology (2018) 49:111–121
https://doi.org/10.1007/s10735-017-9751-2

ORIGINAL PAPER

Reduced myofilament component in primary Sjögren's syndrome salivary gland myoepithelial cells

Margherita Sisto[1] · Loredana Lorusso[1] · Giuseppe Ingravallo[2] · Roberto Tamma[1] · Beatrice Nico[1] · Domenico Ribatti[1,3] · Simona Ruggieri[1] · Sabrina Lisi[1]

Received: 26 October 2017 / Accepted: 30 December 2017 / Published online: 4 January 2018

Abstract
Primary Sjögren's syndrome (pSS) is a solitary poorly understood autoimmune inflammatory disease by involvement of the salivary and lacrimal glands resulting in dry mouth and dry eyes. Myoepithelial cells (MECs) are cells knowing for its hybrid epithelial and mesenchymal phenotype that are important components of the salivary gland (SGs) structure aiding the expulsion of saliva from acinar lobules. In this study we investigate possible alteration in the myofilament component of MECs in SGs specimens obtained from pSS patients in comparison with healthy subjects, to evaluate MECs hypothetical involvement in the pathogenesis of pSS. The expression of alpha-smooth muscle actin (α-SMA) and p63, as MECs markers, was evaluated in bioptic specimens from pSS and healthy labial SGs through immunohistochemistry and immunofluorescence analyses; the distribution of MECs markers was quantified using Aperio ScanScope and ImageScope software to provide quantitative assessments of staining levels. Our observations demonstrated that p63 nuclear labeling in pSS MECs is preserved whereas α-SMA cytoplasmic staining is strongly and significantly reduced when compared with healthy SGs; the digital images analysis quantification of the expression of labeled α-SMA and p63 protein in the healthy and pSS MECs salivary tissues, led to results suggesting a loss of mechanical support for acini and ducts in pSS, correlated, probably, with the reduction of salivary flow that features one important aspect of pSS disease.

Keywords Sjögren's syndrome · Salivary glands · Myoepithelial cells · α-SMA · P63

Introduction

Sjögren's syndrome (SS) is a complex systemic autoimmune progressive disease that primarily affects several exocrine glands and leads to their functional impairment (Vitali et al. 2002; Vitali 2003; Delaleu et al. 2005; Lee et al. 2009; Voulgarelis and Tzioufas 2010). SS occurs either independently as a primary disease (pSS) or as a secondary to other autoimmune rheumatic diseases (Ramos-Casals and Font 2005). The exocrine gland involvement, primarily salivary (SGs) and lacrimal glands, is characterized by a focal, mononuclear cell infiltrate which is accumulated around ducts causing dysfunction and structural damage (Moutsopoulos 1994). pSS is clinically characterized by dryness of the eyes and mouth due to a strong reduction, either qualitatively or quantitatively, in fluid secretion by lacrimal glands and SGs that negatively impact on oral health. The histopathological characteristics of the minor SGs in pSS disease include a decrease or disappearance of acini, lymphocytic infiltration and hyperplasia of the lining cells of the intraglandular ducts. The destruction of acinar cells, that represent the only water-permeable portion of the gland and are central to the initiation of fluid movement in the secretion process, could be implicated in the SS saliva impairment (Delporte et al. 2016). In the SGs, epithelial ductal and acinar structures are surrounded by a contractile myoepithelial cells (MECs) layer. MECs are multipolar stellate cells possessing many flat processes and closely related to the secretory units and proximal ducts, located between the basal lamina and the

✉ Margherita Sisto
margherita.sisto@uniba.it

[1] Department of Basic Medical Sciences, Neurosciences and Sensory Organs (SMBNOS), Section of Human Anatomy and Histology, University of Bari "Aldo Moro", piazza Giulio Cesare 1, 70124 Bari, Italy

[2] Department of Emergency and Organ Transplantation (DETO), Pathology Section, University of Bari "Aldo Moro", Bari, Italy

[3] National Cancer Institute "Giovanni Paolo II", Bari, Italy

acinar or ductal cells (Chitturi et al. 2015; Balachander et al. 2015; Shah et al. 2016). Distribution of MECs varies considerably between types of glands and even in the same gland during the course of development (Shear 1966; Young and Van Lennep 1977; Sato et al. 1979). The morphology of these cells could be also variable and their role includes contraction when the secretory function of the gland is stimulated, compressing and strengthening the cells of the glandular parenchyma and assisting the expulsion of saliva. MECs resemble smooth muscle and epithelial cells, which determines the complexity of their biological functions (Raubenheimer 1987; Raubenheimer et al. 1987; Redman 1994).

Electron microscopic analyses showed that the MECs cytoplasm is filled with thin myofilaments arranged in parallel and resulted immunoreactive for alpha-smooth muscle actin (α-SMA) (Ianez et al. 2010). MECs contain various contractile proteins such as myosin, calponin, and caldesmon, in addition to α-SMA (Foschini et al. 2000). The shape of the MECs suggest that their contraction might reduce the luminal volume in glandular acini, and these cells may play a role in expelling secretory products from acini to the excretory ducts which was later demonstrated experimentally (Chitturi et al. 2015). Recently, loss of MECs has been reported in sialadenosis patients (Ihrler et al. 2010) and in parotid glands of diabetic NOD mice (Nashida et al. 2013). Even in our recent investigation, we suggested that the capacity for water flow across the membrane of MECs may be altered in pSS, since aquaporin 4 (AQP4) expression in these cells resulted selectively decreased in comparison with the expression in healthy subjects (Sisto et al. 2017). The presence of AQP4 on SGs MECs, allowing water inflow and outflow through MECs membrane, raises the possibility that some phases of salivary secretion may be mediated indirectly through an action of MECs on the acinar and ductal cells. The strong down-regulation of AQP4 expression in pSS MECs demonstrates that these cells do not function normally in pSS glands, and therefore some phases of salivary secretion may be impaired (Sisto et al. 2017).

Actually, there is very limited knowledge concerning the pathological processes underlying xerostomia and reduced salivary flow. Given the importance of MECs in SGs physiology and to better evaluate this, we supposed that MECs might decrease or shrink in pSS SGs. To test this hypothesis, we used salivary biopsy specimens obtained from patients with well-defined pSS comparing them with healthy controls, to assess the expression of MECs differentiation markers; given the mixed epithelial and smooth muscle phenotype of MECs, and the need to distinguish the MECs layer from myofibroblasts, ductal or acinar epithelial cells, and vascular smooth muscle, most of the immunohistochemical ideal markers used must possess high sensitivity and specificity. At present, Abs against α-SMA, the major cytoplasmic smooth muscle contractile protein, and against the nuclear protein p63, are commonly used to molecularly identify of MECs (Longtine et al. 1985; Egan et al. 1987; Gugliotta et al. 1988; Foschini et al. 2000; Barbareschi et al. 2001; Reis-Filho and Schmitt 2002; Bilal et al. 2003; Ianez et al. 2010).

We observed loss of the myofilament compartment in pSS MECs, suggesting that MECs function might be compromised in pSS salivary tissues and correlates, probably, with the reduction of saliva flow that features one important aspect of this disease.

Materials and methods

Patient selection and characteristics

The Department of Pathology, University of Bari Medical School, has selected 32 bioptic specimens of pSS labial SGs (LSGs) (61.3 ± 1.2 years old) according to the developed 2016 ACR/EULAR classification criteria for pSS (Shiboski et al. 2016) that are based on the weighted sum of five items: anti-SSA/Ro antibody positivity and focal lymphocytic sialadenitis with a focus score of ≥ 1 foci/4 mm^2, each scoring 3; an abnormal ocular staining score of ≥ 5 (or van Bijsterveld score of ≥ 4), a Schirmer's test result of ≥ 5 mm/5 min, and an unstimulated salivary flow rate of ≥ 0.1 ml/min, each scoring 1. LSGs were harvested from the lower lip under local anesthesia through normal mucosa, according to the explant outgrowth technique (Sens et al. 1985). Healthy volunteers (55.3 ± 0.98 years old, N = 10) with no salivary condition and which had a normal salivary biopsy were included in this experimental procedure as controls. Informed consent from all the subjects and approval by the local ethics committee was obtained. Tissue destined for immunohistochemistry was cut into small pieces and the tissue blocks were then embedded in paraffin and sectioned at 3 µm thickness.

Immunohistochemical staining method for MECs markers expression

Serial 3 µm sections of healthy and pSS formalin-fixed, paraffin-embedded LSGs tissues were used for immunohistochemical staining. While rehydrating the deparaffinized sections in graded al-cohol, the slides were immersed for 1 h in 70% ethanol supplemented with 0.25% NH3, and rehydration was resumed by immersion in 50% ethanol for 10 min. After deparaffinization and dehydration, the slides were washed in phosphate-buffered saline (PBS) (pH 7.6 3 × 10 min), then immersed in EDTA buffer (0.01 M, pH 8.0) for 20 min in water bath at 98 °C to unmask antigens. The sections were immunolabelled according to the following

procedure: blockade of endogenous peroxidase by treatment with 3% hydrogen peroxide solution in water for 10 min at room temperature (RT); rinsing for 3 × 10 min in PBS, pH 7.6; pre-incubation in non-immune donkey serum (Dako LSAB kit, Dako, CA, USA) for 1 h at RT; incubation overnight at 4 °C with primary antibodies (Abs) and dilutions were done as follows: rabbit anti-human-α-SMA Ab (1:100 dilution, Abcam, Abcam, Cambridge, UK), mouse anti-human-p63 Ab (1:100 dilution, Dako, CA, USA), mouse anti-human calponin mAb (1:300 dilution, Dako, CA, USA). The sections were washed for 3 × 10 min in PBS and after incubated with the related secondary Abs (Santa Cruz Biotechnology, TX, USA) diluted 1:200 in PBS for 1 h at RT; rinsing for 3 × 10 min in PBS; incubation with the streptavidin-peroxidase complex (Vector Laboratories, CA, USA) for 1 h at RT; incubation with the chromogen 3,3-diaminobenzidine tetrahydrochloride (DAB) (Vector Laboratories) for 10 min at RT, counterstained with hematoxylin (Merck Eurolab, Dietikon, Switzerland). Negative controls of the immunoreactions were performed by replacing the primary Ab with donkey serum diluted 1:10 in PBS. After the addition of the secondary Ab, no specific immunostaining was observed in the negative controls (data not shown). Therefore, immunohistochemical double-staining with the primary Abs above reported was performed to study the co-localization of p63 and α-SMA in pSS and in healthy MECs.

Immunofluorescence labelling and confocal microscopy study

Immunofluorescence analysis was performed using deparaffinized sections from pSS LSGs biopsies with high grade of inflammation. Immunolabelling was carried out using primary Abs, that were mouse anti-human p63 protein (Dako, CA, USA) and rabbit anti human α-SMA (Abcam, Cambridge, UK). The sections were immersed for 30 min in blocking buffer (PBS, 1% BSA, 2% FCS); 30 min in PBS and incubated with primary Abs over night at 4 °C. Next, primary antibodies were detected with the appropriate secondary Abs Alexa Fluor 488 donkey anti-mouse IgG, diluted 1:200 in PBS (Molecular Probes, Life Technologies) for anti-human p63 protein and Alexa Fluor 568 goat anti-rabbit IgG conjugate, diluted 1:200 in PBS (Molecular Probes) for anti human α-SMA. The sections were drained and coverslipped in Vectashield anti-fade mounting medium (Vector Laboratories). Controls were performed by omitting either one or both primary Abs or by using inappropriate secondary Abs. All controls gave no detectable labelling (data not shown). The sections were observed under a Leica TCS SP confocal laser scanning microscope using ×40 and ×63 oil-immersion objective lenses with either ×1 or ×2 zoom factors. On the immunolabelled sections, a sequential image acquisition was applied of the two fluorophores, Alexa Fluor 488 (excitation at 488 nm and detection range 500–535 nm; green fluorescence) and Alexa Fluor 568 (excitation with 568 nm and detection range 580–620 nm; red fluorescence). Confocal images were taken at 0.5-µm intervals through the z-axis.

Aperio digital immunohistochemistry analysis and quantification

All slides were scanned using high-resolution digital Aperio Scanscope CS2 (Leica Biosystems, Nussloch, Germany) and stored as digital high resolution images on the workstation associated with the instrument. Digital slides were analyzed with Aperio ImageScope v.11 software (Leica Biosystems) at ×10 magnification and ten fields with an equal area were selected for the analysis at ×40 magnification by systematic random sampling (Jannink et al. 1995). α-SMA, p63 and calponin proteins expression were assessed with the Positive Pixel Count algorithm embedded in the Aperio ImageScope software and reported as positivity percentage, defined as the number of positively stained pixels on the total pixels in the image. This approach provides a reliable automatic estimation of the amount of stained structures in the tissue and is less sensitive to errors linked to high cell densities when compared to methods involving direct cell counting (Rizzardi et al. 2012).

ImageJ digital immunofluorescence analysis and quantification

For immunofluorescent image quantification, representative areas of the sections were viewed using a ×20 objective and photographed using a Zeiss AxioCam HRc (Zeiss, Oberkochen, Germany). For each image of stained slides, ten representative visual fields, each 586 µm x 439 µm in area, were randomly selected from sections of all tissue specimens under study and analysed using a computerized morphometric analysis software (ImageJ, version 1.46c; WS Rasband, National Institutes of Health, Bethesda, MD, USA, http://rsb.info.nih.gov/ij/). MECs cell bodies were identified by their nucleus and morphology on each of the selected stained sections and these cells were counted on the captured images; the number of MECs positive for each immunoreactions and the area occupied by these cells were measured. Positive areas were expressed as percentage of the total tissue area examined [percentage positive pixels (PPP)]. Data were expressed as mean ± standard error of the mean (SE).

Statistical analysis

All measurements were calculated as mean percentage ± SE. Statistical analysis was performed using Microsoft Excel 2007 software. Differences among groups were determined

using T-test and statistical differences were considered to be significant if $p \leq 0.05$. All experiments were performed a minimum of three times.

Results

Characterization of MECs markers

Because MECs are not always readily identifiable on routine haematoxylin and eosin stained sections, many immunohistochemical methods have been used to highlight an intact and functional MECs layer. In this experimental procedure, to confirm that MECs were detectable in SGs of pSS patients and healthy subjects, we used a combination of immunohistochemical stains to investigate the expression of α-SMA and p63 proteins known to be enriched in MECs. As reported in Fig. 1, showing both healthy (panels a, b for α-SMA and e, f for p63) and pSS (panels c, d for α-SMA and g, h for p63) LSG sections, α-SMA is localized in the cytoplasm; in contrast, p63 was restricted in basal cell nuclei and the signal for all two markers was enriched in cells that ensheath or are closely associated with acinar and ductal epithelial cells of healthy and SS SGs. The presence of stained cells in these anatomical locations was consistent with the established distribution of MECs. Thus, we concluded that our staining protocols effectively detected MECs in human salivary tissues (Fig. 1).

Alpha-SMA protein expression decrease in SS MECs salivary tissues

In order to investigate the possibility that a loss of myofilament component and consequently of the contractile function of the MECs could be involved in the decreased salivary secretion in pSS, we firstly performed immunohistochemical analysis using anti-human α-SMA and anti-human nuclear p63 Abs, on salivary gland biopsy specimens obtained from patients affected from pSS and comparing them with those obtained from healthy controls (Fig. 1). Immunohistochemical analysis revealed that in normal healthy SGs, no α-SMA staining was observed in the acinar and ductal cells, but a strong α-SMA labeling signal is restricted to the cytoplasm of the MECs located on the basal surface of acinar

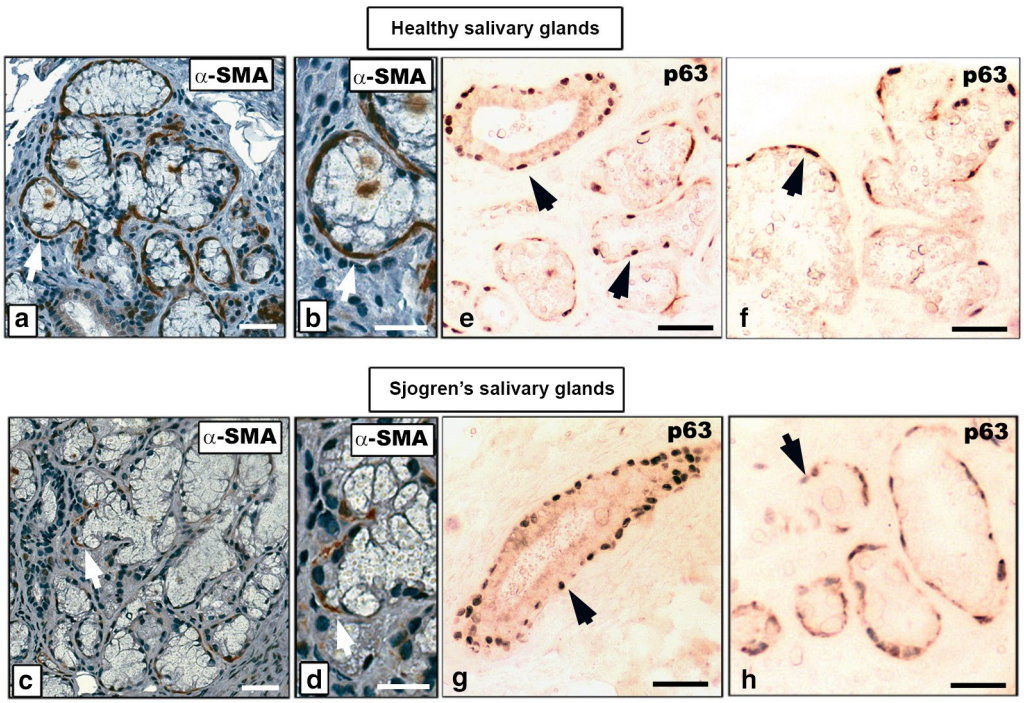

Fig. 1 Immunohistochemical localization of α-SMA in healthy (**a, b**) and pSS (**c, d**) salivary biopsy and, p63 in healthy (**e, f**) and pSS (**g, h**) salivary tissues. Immunohistochemical analysis revealed α-SMA labelling in the cytoplasm of the MECs that surround acinar and ductal cells in healthy (**a, b**) and pSS (**c, d**) salivary biopsies. A strong positivity for α-SMA was detected in MECs of healthy salivary sections (**a, b**) and the intensity of labeling was strongly reduced in pSS MECs (**c, d**). The images **b** and **d** represent a high magnification of acini of sections derived from healthy and pSS salivary gland biopsies, respectively. p63 nuclear labeling in the MECs is preserved with same intensity both in healthy (**e, f**) and pSS (**g, h**) salivary tissues. Brown staining shows positive immunoreaction; blue staining shows nuclei. No counterstain in **e–h** images. Black arrowheads indicate the nuclei of the MECs while white arrowhead show α-SMA expression in the cytoplasm of the MECs. **a, c** original magnification, ×20; **b, d–h** original magnification, ×40; α-SMA, α-smooth muscle actin. *MECs* myoepithelial cells. Bar 20 µm

and ductal cells as a thin layer, and diffusely distributed in the cytoplasmic flat processes that extend between and over the acinar and ductal lining cells (panels a, b). Compared to control subjects, in pSS patients' salivary tissues (panels c, d), the α-SMA cytoplasmic distribution was heavily reduced or almost completely absent in pSS MECs and interestingly, the brown signal was confined and narrowed around nuclei of MECs. Therefore, α-SMA labeling is absent in the cytoplasmic processes of MECs that radiate and embrace the secretory unit. Thus, subsequently, we focused our attention on p63 protein nuclear immunolocalization in pSS patients and healthy subjects. Figure 1 illustrates the sections of healthy (panels e, f) and pSS bioptic tissues (panels g, h) stained with anti-human p63 Ab. p63-reactive nuclei were seen in the cells surrounding the acinar and ductal cells and the localization of these p63-reactive nuclei suggested that the p63-reactive cells are effectively MECs. Luminal duct cells and acinar cells were unreactive. The observed intense nuclear p63 immunoreactivity in the elongated nuclei of the healthy MECs (panels e, f) did not differ from that observed in pSS MECs (panels g, h). This represents a very intriguing observation because suggests that no difference seems to be found in the total number of p63-positive MECs between healthy and pSS SGs; what instead is clearly evident is a reduction of myofilaments component in pSS MECs. To confirm and expand the observations of MECs differentiation markers loss within pSS MECs, we performed an immunohistochemical analysis of the expression of calponin, an actin-binding protein that regulates the power stroke during smooth muscle contraction (Haeberle 1994; Matthew et al. 2000), in healthy and pSS biopsies (Fig. 2).

We found MECs expression of this marker to vary between healthy individual and pSS patients and a clear reduction of calponin expression was observed in the MECs

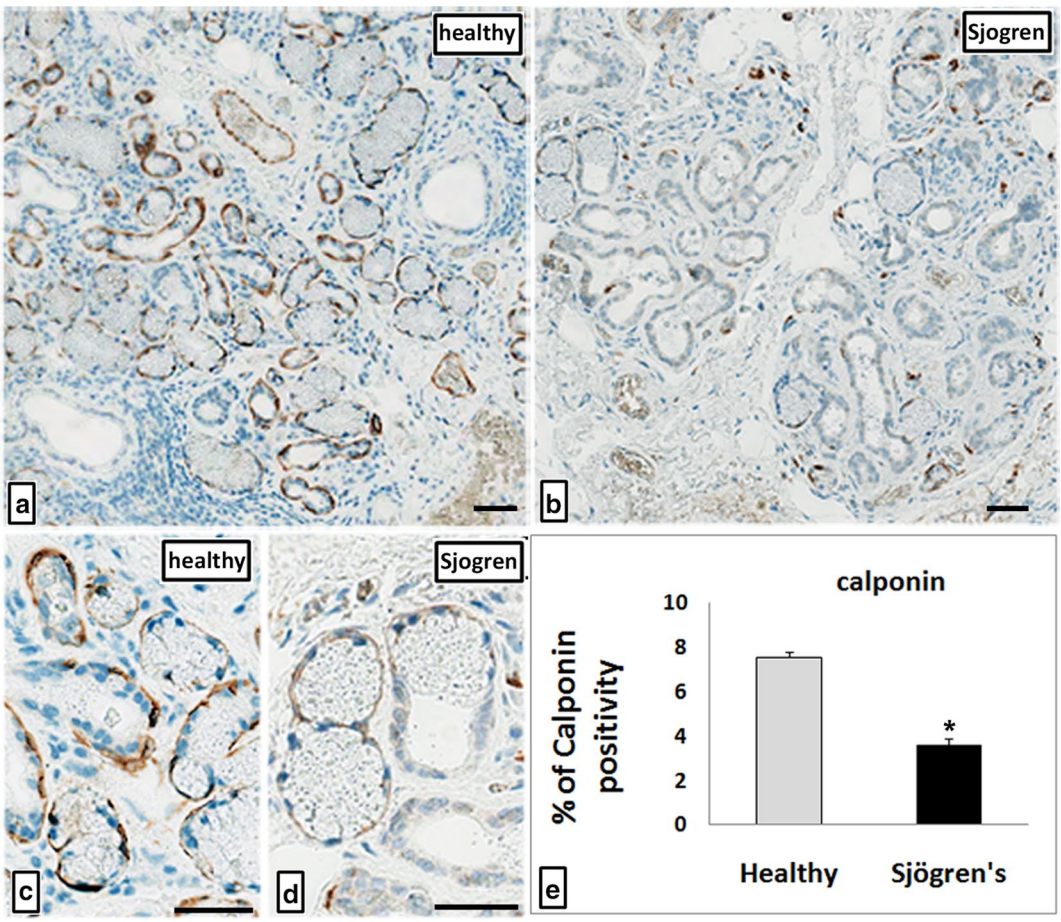

Fig. 2 Immunohistochemical localization of calponin in healthy (**a, c**) and pSS (**b, d**) salivary biopsies. Immunohistochemical analysis revealed calponin labelling in the cytoplasm of the MECs that surround acinar and ductal cells in healthy (**a, c**) and pSS (**b, d**) salivary tissues. A strong positivity for calponin was detected in MECs of healthy salivary sections (**a, c**) and the intensity of labeling was strongly reduced in pSS MECs (**b, d**). The images **c** and **d** represent a high magnification of acini of sections derived from healthy and pSS salivary gland biopsies, respectively. Immunohistochemistry signal quantification of calponin positivity (**e**) on the sections obtained from healthy and pSS salivary tissues using the Aperio ImageScope Software. *$p < 0.01$. Brown staining shows positive immunoreaction; blue staining shows nuclei. **a, b**, original magnification, ×20; **c, d**, original magnification, ×40; Bar 20 µm

of pSS patients (Fig. 2, panels b, d) in comparison with panels a, c, representing healthy SGs specimens. Cumulatively, these data are consistent with the hypothesis that MECs function could be compromised in this inflammatory chronic condition. The expression of labeled calponin protein in the healthy and pSS MECs obtained by Aperio scanscope, was also quantified using the computerized morphometric analysis software and express in terms of pixel/intensities (Fig. 2, panel e) demonstrating a significant ($p < 0.01$) reduction of calponin expression in pSS biopsies.

To confirm the decreased density of the distribution of the myofilament component of pSS MECs, a double immunohistochemistry was carried out incubating the sections with a cocktail of antibodies (p63 and α-SMA) to determine the contemporary distribution and immunolocalization of these proteins and to make a comparison by Aperio digital immunohistochemistry analysis between healthy (Fig. 3) and pSS MECs (Fig. 4).

We found that almost all of the MECs of healthy salivary tissues with positive nuclear p63 reactivity co-expressed α-SMA cytoplasmic staining (Fig. 3, panels a–f). As expected, in pSS tissues (Fig. 4, panels a–f), it notes that MECs p63 nuclear labeling is retained whereas α-SMA cytoplasmic staining is strongly reduced validating the hypothesis of a loss of myofilament component in pSS MECs.

Quantitative comparison of α-SMA and p63 immunohistochemical staining measured by digital image analysis

To quantify the expression of labeled α-SMA and p63 protein in the healthy and pSS MECs, the digital slide images obtained by Aperio scanscope were viewed and analyzed in terms of pixel/intensities using the computerized morphometric analysis software (Fig. 5).

The data revealed a significant difference in the percentage of strong positive pixels for α-SMA protein in the MECs of healthy and pSS salivary tissues ($p < 0.01$). In detail, the healthy salivary tissues showed the highest percentage of strong α-SMA positive pixels (mean 8.87 ± 0.34) when compared to the pSS (mean 3.49 ± 0.27) while percentage of strong positive pixels for p63 showed the similar percentage for both pSS (mean 5.97 ± 0.06) and healthy salivary MECs (mean 6.28 ± 0.02). (Graphs reported in the Fig. 5).

Thus, we found a significant ($p < 0.01$) reduction in the α-SMA expression in pSS MECs in comparison with healthy MECs, concordant with the microscopic observation. The decreased myofilament component observed in pSS MECs represents an important breakthrough, supporting the opinion that MECs which participate to the release of saliva by covering acini and ducts with their contractile processes, could be defective in pSS. The

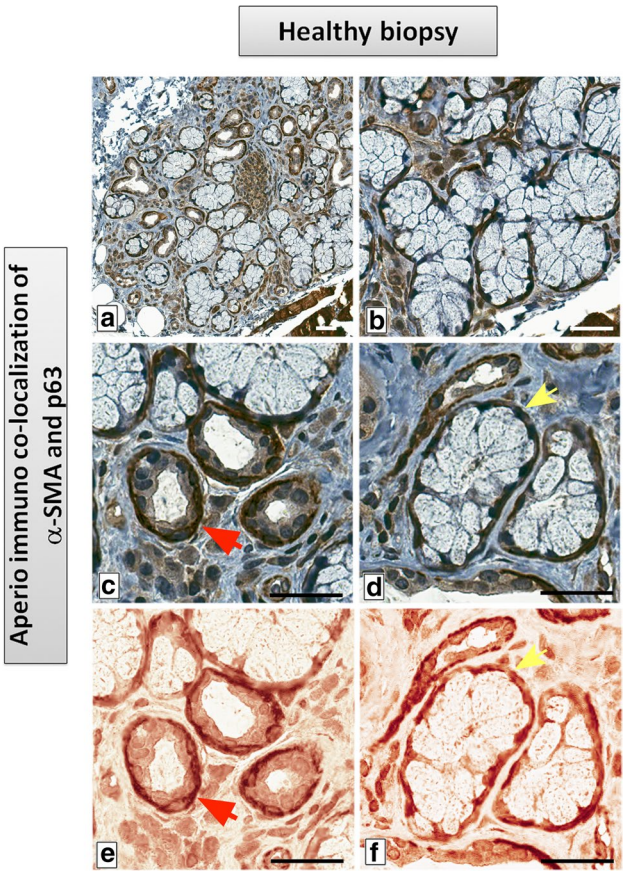

Fig. 3 Double immunohistochemistry for α-SMA and p63 in healthy salivary glands. The representative images **a–d** show α-SMA and p63 immuno co-localization in the MECs. The magnified images **c, d** show a wide cytoplasmic distribution of α-SMA protein expression in the MECs and p63 restrictive expression in the nuclei of the same cell. **a** original magnification, ×10; **b** original magnification, ×40; **c, d** original magnification, ×100. No counterstain was applied in **e, f** images. The slides were scanned and analyzed with Aperio ImageScope instrument. Yellow arrowhead indicates the nuclei of the MECs while red arrowhead shows α-SMA expression in the cytoplasm of the MECs. α-SMA, α-smooth muscle actin. *MECs* myoepithelial cells. Bar 10 µm. (Color figure online)

pseudo-color markup images (Fig. 6, panels b, d) are representative screenshots images of two whole slides, double immunostained for α-SMA and p63, derived from healthy (a) and pSS (c) salivary glands and analyzed by Aperio's ImageScope. The markup images represent an algorithm elaboration in order to evaluate the p63 nuclear immunolocalization. The positive pixels are represented in red spots and the negative pixels are shaded blue. These images show as the p63 positivity evaluation is specific in both healthy (b) and pSS MECs (d) confirming the conclusion that p63 nuclear labeling presents similar levels of expression between healthy and pSS MECs whereas α-SMA cytoplasmic staining is strongly reduced in pSS.

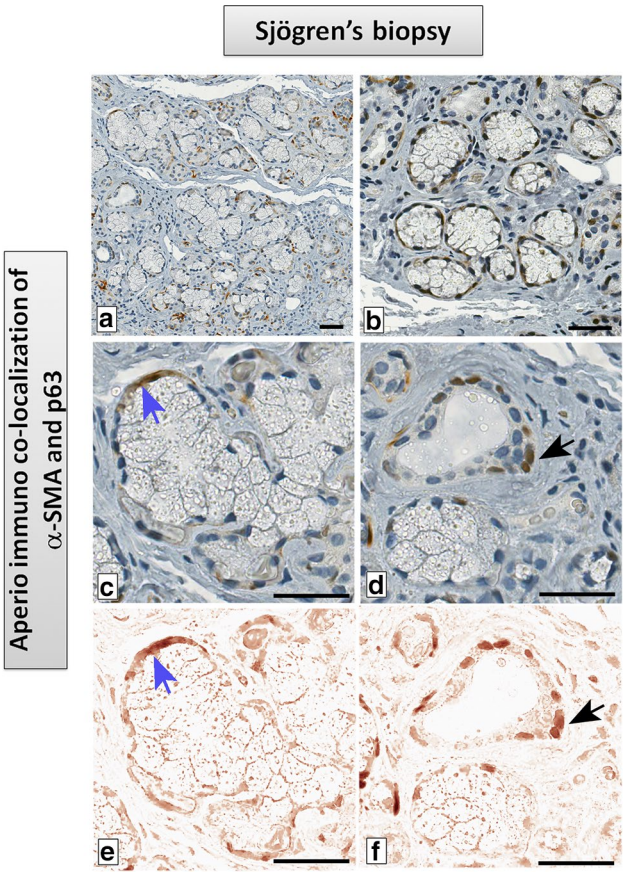

Fig. 4 Double immunoperoxidase stain for α-SMA and p63 in the pSS salivary glands. The representative images **a**–**d** show α-SMA and p63 immuno co-localization in the MECs. The magnified images **c, d** show a reduced distribution of α-SMA protein expression in the cytoplasm while p63 labelling intensity preserved in the nuclei of the MECs. **a** original magnification, ×10; **b** original magnification, ×40; **c, d** original magnification, ×100. No counterstain was applied in **e, f** images. Images were scanned analyzed with Aperio ImageScope instrument. Black arrowhead indicates the nuclei of the MECs while blue arrowhead shows α-SMA expression in the cytoplasm of the MECs. *α-SMA* α-smooth muscle actin. *MECs* myoepithelial cells. Bar 10 µm. (Color figure online)

Immunofluorescence confocal microscopy confirmed myofilament component deficiency in pSS MECs

To more directly determine the precise subcellular localization of α-SMA and p63 nuclear protein in MECs and to confirm that α-SMA expression varies between pSS patients and healthy donors and resulted lower in pSS patients than in controls, sections of healthy and pSS salivary gland were labeled with antibodies to human α-SMA and p63, and viewed by high-resolution confocal microscopy by immunofluorescence (Fig. 7A). Figure 7A shows labelling of α-SMA (red) and p63 (green) in sections derived from healthy (panels a, c) and pSS samples (panels b, d). As depicted, α-SMA was located diffusely in the cytoplasm of MECs adjacent to the acinar epithelial cells and intercalated duct, while p63 labelling is selectively expressed in the nuclei of the MECs. As expected, and confirming immunohistochemistry results, α-SMA protein expression resulted strongly decreased in the pSS MECs (panel b) in comparison with healthy samples sections (panel a), while p63 labeling signal is conserved (respectively panel c, for healthy controls and d for pSS). This result confirms that the total number of MECs is not altered in pathological condition pSS, but, however, in the myoepithelium layer of pSS salivary tissues injuries occur that compromise the function and structural integrity of the MECs stratum. With ImageJ software, quantitative and statistical analyses were carried out on immunofluorescence images to measure changes in α-SMA and p63 proteins expression between healthy and pSS MECs (Fig. 7 B, C). Quantification of confocal microscopy images led to similar results to those obtained by immunohistochemistry and Aperio scanscope computerized morphometric analysis software.

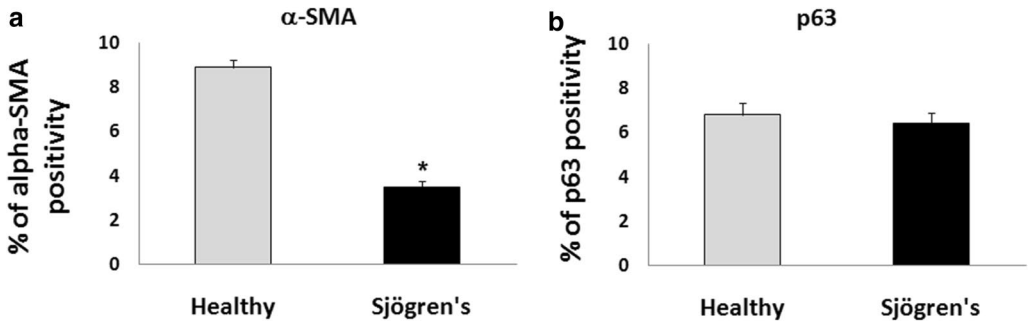

Fig. 5 Immunohistochemistry signal quantification of α-SMA positivity (**a**) and p63 positivity (**b**) on the sections obtained from healthy and pSS salivary tissues using the Aperio ImageScope Software. *$p < 0.01$. *α-SMA* α-smooth muscle actin

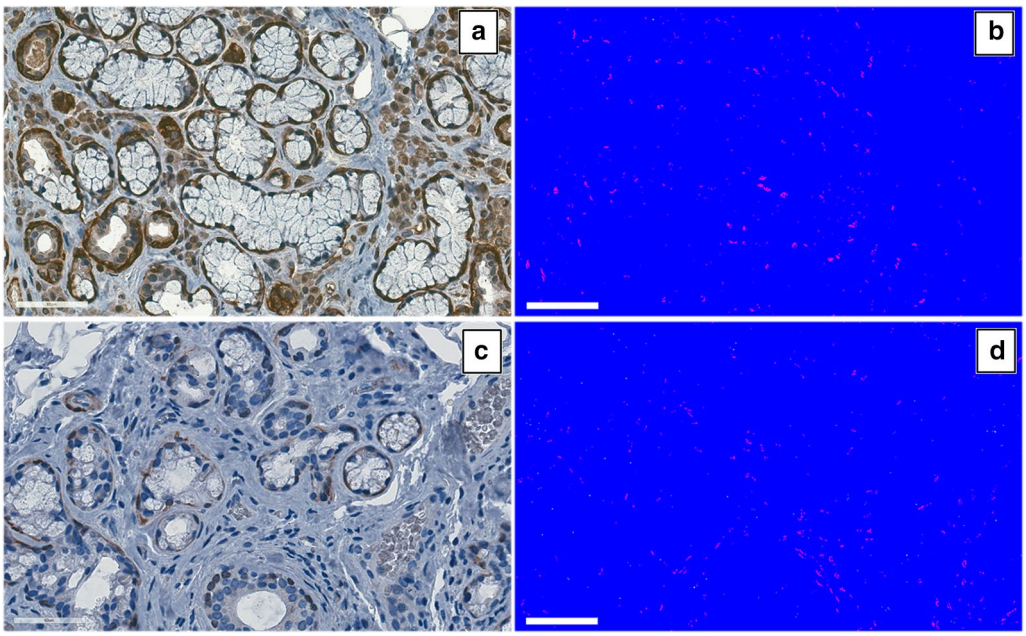

Fig. 6 Representative screenshots images of two whole slides, double immunoperoxidase stained for α-SMA and p63, derived from from healthy (**a**) and pSS (**c**) salivary glands as seen in Aperio's ImageScope viewer application after their scan. **b, d** represent pseudo-color markup images obtained from the original images (**a–c**) as an algorithm elaboration in order to evaluate the p63 nuclear immunolocalization. The positive pixels are represented in red and the negative pixels are shaded blue. The markup images show as the p63 positivity evaluation is specific in both healthy (**b**) and pSS MECs (**d**). Bar 60 µm. (Color figure online)

Discussion

MECs are important components of salivary gland structure, and their contractile function, due to the presence of myofilament proteins, helps the secretory activity of the gland, compressing and strengthening the cells of the glandular parenchyma and assisting the expulsion of saliva. Xerostomia and hyposalivation are the most common symptoms of pSS associated to the loss of salivary gland function. Actually, modern sophisticated microscopic techniques have resulted in a surge of new information on MECs through specific markers which facilitated studies on their presence and behavior in disease processes. We focused our studies on two MECs markers: α-SMA and p63, commonly used to identify the MECs, in healthy controls and pSS LSGs biopsies by means of immunohistochemistry, high-resolution confocal microscopy and quantitative image analyses.

The most striking observation, revealed by immunohistochemistry and immunofluorescence results, was that the α-SMA protein labelling, widely diffused in the cytoplasm and in the flat process that embrace the acinar cells of the secretory unit, was remarkably less intense in the MECs of SGs of patients with pSS in comparison of healthy subjects. In the acinar cells and ductal cells α-SMA labelling was absent. Further, our investigations were highly upgrade by data obtained from a double immunohistochemistry carried out incubating the sections contemporary with the same biomarkers, to determine the distribution and immuno co-localization of these proteins within the MEC, in healthy and pSS salivary tissues. We found that almost all the MECs of healthy salivary tissues with positive nuclear p63 reactivity co-expressed α-SMA cytoplasmic staining. In pSS tissues, it is significant to note that p63 nuclear labeling in MECs is preserved whereas α-SMA cytoplasmic staining is strongly and significantly reduced, validating the hypothesis of a loss of myofilament component in MECs of pSS patients. A quantification of the expression of labeled α-SMA and p63 protein in the healthy and pSS MECs salivary tissues was performed using Aperio digital IHC analysis that confirmed a significant difference in the percentage of strong positive pixels for α-SMA protein in the MECs of healthy salivary tissues when compared to the pSS, while p63-positive MECs showed the similar percentage between pSS and healthy salivary tissues.

To determine and further explore the precise subcellular localization of these myoepithelial biomarkers, we performed an immunofluorescence staining and the images were observed by high-resolution confocal microscopy. Immunolabeling confirmed the expression of cytoplasmic α-SMA and nuclear p63 in healthy and pSS MECs. As expected, the α-SMA labeling distribution resulted significantly decreased in the cytoplasm of the pSS MECs in comparison with healthy MECs, whereas the levels of nuclear localized p63 showed similar trends of expression

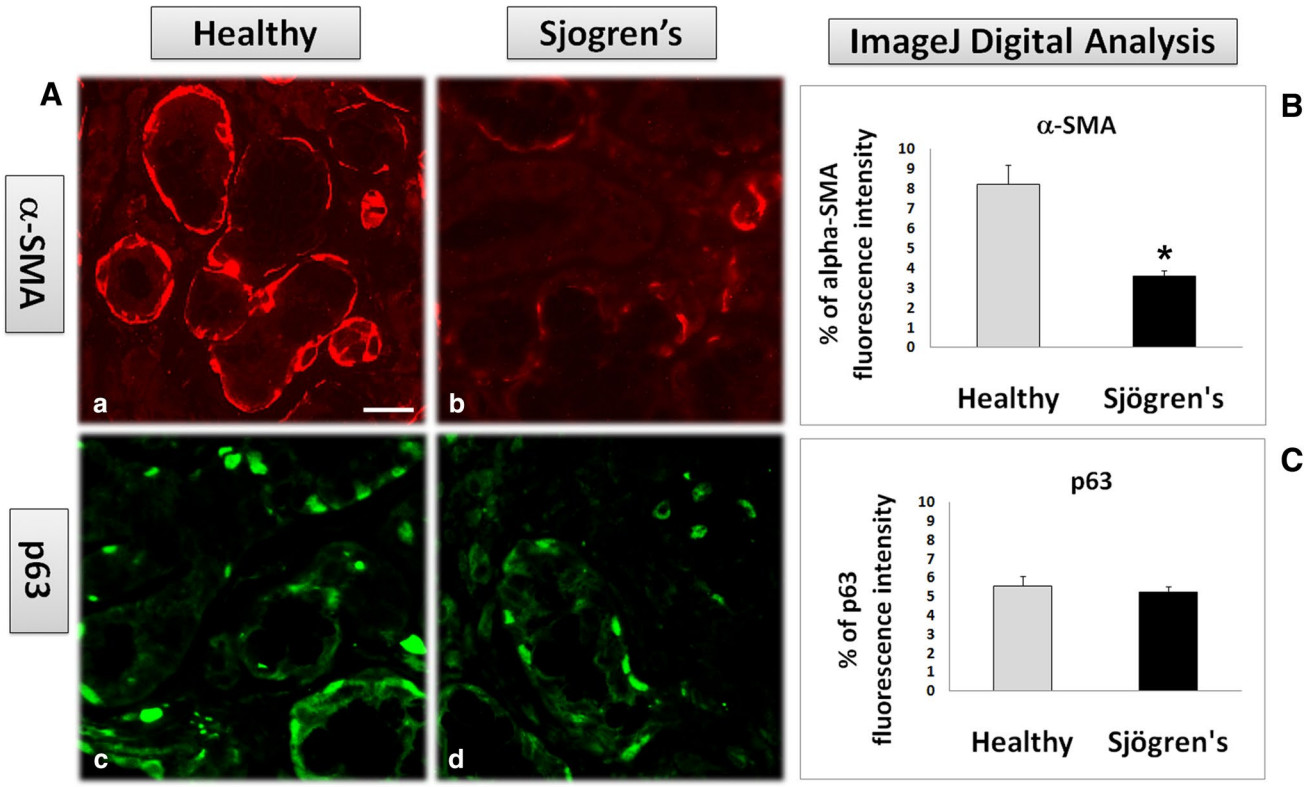

Fig. 7 **A** Immunofluorescence staining of α-SMA (red) and p63 (green) in MECs from healthy (**a, c**) and pSS salivary gland biopsies (**b, d**). Immunofluorescence analysis showed that MECs of acini and ducts were strongly positive for α-SMA and p63 in healthy conditions (**a, c**) while in pSS an evident decrease of α-SMA-positive MECs was observed (**b**). p63 labeling expression is preserved in pSS MECs (**d**). **B, C** Quantification of the percentage of α-SMA and p63 immunofluorescence intensity in MECs compared with healthy and pSS salivary tissues. Images were analyzed with ImageJ software. Bar 10 µm. *$p < 0.01$. (Color figure online)

in healthy and pSS salivary tissues. Quantifying p63 expression revealed by immunofluorescence, in fact, there was not a significant decrease in positivity of p63-positive MECs in pSS as compared with the healthy MECs, suggesting that the number of MECs is not altered and results obtained could be interpreted as evidence of injured MECs in pSS salivary gland tissues. Intriguingly, the remarkable reduction of expression of α-SMA occurred in pSS MECs, it is consistent with the notion that myoepithelium function could be compromised in the myofilament component hallmark of the contractile activity of the salivary gland of pSS patients and becoming unable to sustain the saliva secretion by contraction. Thus, the far greater, major decrease in the density of the distribution of the myofilament component indicates that there is a major decrease of the contractile myofibril component within the MECs that mechanically support the acini, and the major atrophy of the myofibril component would result in a loss of this function.

Until recently, it has been widely demonstrated that the loss of salivary function seen in pSS occurred as a direct consequence of salivary gland atrophy, including fibrosis, acinar cell atrophy and ductal cell hyperplasia (Nikolof and Illei 2009). Although the severe impairment in salivary secretion in pSS is thought to be related to the extent of lymphocytic infiltration and subsequent loss of glandular tissue, lymphocyte infiltration alone is not sufficient to explain the altered secretory function observed in pSS patients (Hayashi 2011).

The significance of MECs in the pathophysiology of pSS is actually unclear. Our recent investigation evidenced a remarkable down-regulation of AQP4 expression in pSS salivary MECs in comparison with healthy glands, giving strong support to the notion that the AQP-dependent mechanism of the rapid control of MECs volume, required to enable these cells to provide structural support during salivary secretion, was altered in pSS glands, and therefore some phases of salivary secretion may be impaired (Sisto et al. 2017).

The fact that MECs are closely related to the secretory units and proximal ducts was also supported from recent studies demonstrating that loss of MECs has yet been reported in sialadenitis (Ihrler et al. 2010); furthermore, recently, a significant reduced α-SMA and AQP8 in MECs of parotid glands of non-obese diabetic (NOD) mice was

demonstrated, leading to SGs hypofunction compared with control mice. Fewer or atrophied MECs observed in diabetic NOD mice imply the importance of these cells in SGs physiology (Wellner et al. 2006; Nashida et al. 2013).

Our data herein reported, suggest a possible implication of MECs, by virtue of their location and features, in the altered secretory function of pSS SGs, that it reflected in a remarkable hyposalivation observed in pSS patients. More broadly, our findings could suggest that the loss of salivary gland secretory function in pSS patients may not be directly related to the overt immune activation observed in the disease, but the changes in pSS MECs function may contribute to the deficiency of fluid secretion.

Results obtained could be an explanation of the observation reported by Jonsson and colleagues that the decreased saliva secretion follows the incidence of focal lymphoid infiltration in a delayed manner, and that the local inflammatory microenvironment that replaces the glandular tissue is not sufficient to explain the severe impairment in salivary secretion (Jonsson et al. 2006). In addition, Deshmukh et al. reported that, in the initial stages of the disease, gland dysfunction and hyposalivation did not correlate with the severity of lymphocytic infiltration and inflammatory grade in the salivary gland and changes in secretion occurred without significant progression of inflammation (Deshmukh et al. 2008).

In conclusion, although elucidation of the detailed aetiology and pathogenesis of pSS is dependent on further research, it is thought that the loss of the myofilament component in pSS MECs supports the evidence of an active participation of MECs in facilitating the secretion of saliva from acinar and ductal part of SGs. Further investigation into their role is needed to define the mechanisms of onset of pSS and, hence, proper research and techniques has to be applied to obtain significant knowledge regarding MEC and its role in salivary gland dysfunction characterizing pSS.

Acknowledgements We are grateful to M.V.C. Pragnell, B.A., for critical reading of the manuscript.

Compliance with ethical standards

Conflict of interest The authors declare they have no competing interests.

References

Balachander N, Masthan KM, Babu NA, Anbazhagan V (2015) Myoepithelial cells in pathology. J Pharm Bioallied Sci 7:S190-S193

Barbareschi M, Pecciarini L, Cangi MG, Macri E, Rizzo A, Viale G, Doglioni C (2001) p63, a p53 homologue, is a selective nuclear marker of myoepithelial cells of the human breast. Am J Surg Pathol 25:1054–1060

Bilal H, Handra-Luca A, Bertrand JC, Fouret PJ (2003) P63 is expressed in basal and myoepithelial cells of human normal and tumor salivary gland tissues. J Histochem Cytochem 51:133–139

Chitturi RT, Veeravarmal V, Nirmal RM, Reddy BV (2015) Myoepithelial cells (MEC) of the SGs in health and tumours. J Clin Diagn Res 9:14–18

Delaleu N, Jonsson R, Koller MM (2005) Sjögren's syndrome. Eur J Oral Sci 113:101–113

Delporte C, Bryla A, Perret J (2016) Aquaporins in SGs: from basic research to clinical applications. Int J Mol Sci 17:166–179

Deshmukh US, Ohyama Y, Bagavant H, Guo X, Gaskin F, Fu SM (2008) Inflammatory stimuli accelerate Sjögren's syndrome-like disease in (NZB x NZW)F1 mice. Arthritis Rheumatol 58:1318–1323

Egan MJ, Newman J, Crocker J, Collard M (1987) Immunohistochemical localization of S100 protein in benign and malignant conditions of the breast. Arch Pathol Lab Med 111:28–31

Foschini MP, Scarpellini F, Gown AM, Eusebi V (2000) Differential expression of myoepithelial markers in salivary, sweat and mammary glands. Int J Surg Pathol 8:29–37

Gugliotta P, Sapino A, Macrí L, Skalli O, Gabbiani G, Bussolati G (1988) Specific demonstration of myoepithelial cells by anti-alpha smooth muscle actin antibody. J Histochem Cytochem 36:659–663

Haeberle JR (1994) Calponin decreases the rate of cross-bridge cycling and increases maximum force production by smooth muscle myosin in an in vitro motility assay. J Biol Chem 269:12424–12431

Hayashi T (2011) Dysfunction of lacrimal and salivary glands in Sjögren's syndrome: nonimmunologic injury in preinflammatory phase and mouse model. J Biomed Biotechnol 2011:407031

Ianez RF, Buim ME, Coutinho-Camillo CM, Schultz R, Soares FA, Lourenço SV (2010) Human salivary gland morphogenesis: myoepithelial cell maturation assessed by immunohistochemical markers. Histopathology 57:410–417

Ihrler S, Rath C, Zengel P, Kirchner T, Harrison JD, Weiler C (2010) Pathogenesis of sialadenosis: possible role of functionally deficient myoepithelial cells. Oral Surg Oral Med Oral Pathol Oral Radiol Endod 110:218–223

Jannink I, Bennen JN, Blaauw J, van Diest PJ, Baak JP (1995) At convenience and systematic random sampling: effects on the prognostic value of nuclear area assessments in breast cancer patients. Breast Cancer Res Treat 36:55–60

Jonsson MV, Delaleu N, Brokstad KA, Berggreen E, Skarstein K (2006) Impaired salivary gland function in NOD mice: association with changes in cytokine profile but not with histopathologic changes in the salivary gland. Arthritis Rheumatol 54:2300–2305

Lee BH, Tudares MA, Nguyen CQ (2009) Sjögren's syndrome: an old tale with a new twist. Arch Immunol Ther Exp (Warsz) 57:57–66

Longtine JA, Pinkus GS, Fujiwara K, Corson JM (1985) Immunohistochemical localization of smooth muscle myosin in normal human tissues. J Histochem Cytochem 33:179–184

Matthew JD, Khromov AS, McDuffie MJ, Somlyo AV, Somlyo AP, Taniguchi S, Takahashi K (2000) Contractile properties and proteins of smooth muscles of a calponin knockout mouse. J Physiol 529:811–824

Moutsopoulos HM (1994) Sjögren's syndrome: autoimmune epithelitis. Clin Immunol Immunopathol 72:162–165

Nashida T, Yoshie S, Haga-Tsujimura M, Imai A, Shimomura H (2013) Atrophy of myoepithelial cells in parotid glands of diabetic mice; detection using skeletal muscle actin, a novel marker. FEBS Open Bio 3:130–134

Nikolof NP, Illei GG (2009) Pathogenesis of Sjögren's syndrome. Curr Opin Rheumatol 21:465–470

Ramos-Casals M, Font J (2005) Primary Sjögren's syndrome: current and emergent aetiopathogenic concepts. Rheumatology 44:1354–1367

Raubenheimer EJ (1987) The myoepithelial cell: embryology, function, and proliferative aspects. Crit Rev Clin Lab Sci 25:161–193
Raubenheimer EJ, van Niekerek JP, Hauman CHJ (1987) Salivary myoepithelium: distribution, structure, functions and pathologic proliferations. J DASA 42:631–637
Redman RS (1994) Myoepithelium of SGs. Microsc Res Tech 27:25–45
Reis-Filho JS, Schmitt FC (2002) Taking advantage of basic research: p63 is a reliable myoepithelial and stem cell marker. Adv Anat Pathol 9:280–289
Rizzardi AE, Johnson AT, Vogel RI, Pambuccian SE, Henriksen J, Skubitz AP, Metzger GJ, Schmechel SC (2012) Quantitative comparison of immunohistochemical staining measured by digital image analysis versus pathologist visual scoring. Diagn Pathol 7:42–47
Sato K, Nishiyama A, Kobayashi M (1979) Mechanical properties and functions of the myoepithelium in the eccrine sweat gland. Am J Physiol 237:177–184
Sens DA, Hintz DS, Rudisill MT, Sens MA, Spicer SS (1985) Explant culture of human submandibular gland epithelial cells: evidence for ductal origin. Lab Invest 52:559–567
Shah AAK, Mulla AF, Mayank M (2016) Pathophysiology of myoepithelial cells in SGs. J Oral Maxillofac Pathol 20:480–490
Shear M (1966) The structure and function of myoepithelial cells in SGs. Arch Oral Biol 11:769–780
Shiboski CH, Shiboski SC, Seror R, Criswell LA, Labetoulle M, Lietman TM, Rasmussen A, Scofield H, Vitali C, Bowman SJ, Mariette X (2016) American College of Rheumatology/European League Against Rheumatism classification criteria for primary Sjögren's syndrome: a consensus and data-driven methodology involving three international patient cohorts. Ann Rheum Dis 76:9–16
Sisto M, Lorusso L, Ingravallo G, Nico B, Ribatti D, Ruggieri S, Lofrumento DD, Lisi S (2017) Abnormal distribution of AQP4 in minor SGs of primary Sjögren's syndrome patients. Autoimmunity 50:202–210
Vitali C (2003) Classification criteria for Sjögren's syndrome. Ann Rheum Dis 62:94–95
Vitali C, Bombardieri S, Jonsson R, Moutsopoulos HM, Alexander EL, Carsons SE, Daniels TE, Fox PC, Fox RI, Kassan SS, Pillemer SR, Talal N, Weisman MH (2002) European Study Group on Classification Criteria for Sjögren's Syndrome. Classification criteria for Sjögren's syndrome: a revised version of the European criteria proposed by the American-European Consensus Group. European Study Group on Classification Criteria for Sjögren's Syndrome. Ann Rheum Dis 61:554–558
Voulgarelis M, Tzioufas AG (2010) Current Aspects of Pathogenesis in Sjögren's Syndrome. Ther Adv Musculoskelet Dis 2:325–334
Wellner RB, Redman RS, Swaim WD, Baum BJ (2006) Further evidence for AQP8 expression in the myoepithelium of rat submandibular and parotid glands. Pflugers Arch 451:642–645
Young JA, Van Lennep EW (1977) Morphology and physiology of salivary myoepithelial cells. Int Rev Physiol 12:105–125